Crystal Structures and Magnetic Properties of MCl_4^{2-} (M=Mn(II) and Co(II)) Salts of *m*- and *p*-*N*-Methylpyridinium Nitronyl Nitroxides

Akira Yamaguchi, Tsunehisa Okuno, and Kunio Awaga*

Department of Pure and Applied Sciences, The University of Tokyo, Komaba, Meguro-ku, Tokyo 153

(Received June 27, 1995)

Organic radical cations, 4,4,5,5-tetramethyl-2-(1-methyl-3 or 4-pyridinio)-3-oxide-4,5-dihydro-1*H*-1-imidazolyloxyl (or, *m*- and *p*-*N*-methylpyridinium nitronyl nitroxides, abbreviated as *m*- and *p*-MPYNN$^+$, respectively), were found to crystallize with magnetic counter anions, MCl_4^{2-} (M = Mn^{2+} ($S=5/2$) and Co^{2+} ($S=3/2$)), although the $MnCl_4^{2-}$ salts were rather air-sensitive. X-Ray full-crystal analyses were carried out on the stable $CoCl_4^{2-}$ salts. The structure of (*m*-MPYNN$^+$)$_2$$CoCl_4^{2-}$ crystallizes in the *monoclinic* $P2_1/c$ space group, while that of (*p*-MPYNN$^+$)$_2$$CoCl_4^{2-}$ belongs to the *triclinic* $P\bar{1}$ space group. Although (*m*-MPYNN$^+$)$_2$$MnCl_4^{2-}$ and (*p*-MPYNN$^+$)$_2$$MnCl_4^{2-}$ were not stable enough for an X-ray full data collection, they were indicated to be isostructural to the corresponding $CoCl_4^{2-}$ salts, respectively, by their diffractions of $20 < \theta < 25°$. Variable-temperature magnetic susceptibility measurements reveal a clear contrast between the (*m*-MPYNN$^+$)$_2$$MCl_4^{2-}$ and (*p*-MPYNN$^+$)$_2$$MCl_4^{2-}$ salts. The two (*m*-MPYNN$^+$)$_2$$MCl_4^{2-}$ salts exhibit a ferromagnetic behavior independently of MCl_4^{2-}, which is attributable to a *m*-MPYNN$^+$ dimer. However, the magnetic properties of two (*p*-MPYNN$^+$)$_2$$MCl_4^{2-}$ salts are strongly dependent on the MCl_4^{2-} anion: (*p*-MPYNN$^+$)$_2$$MnCl_4^{2-}$ exhibits an antiferromagnetic interaction in opposition to a ferromagnetic one in (*p*-MPYNN$^+$)$CoCl_4^{2-}$. The magnetic difference between them can be qualitatively understood in terms of a charge-transfer interaction between MCl_4^{2-} and *p*-MPYNN$^+$, in which the difference in the electronic structure between the Mn^{2+} and Co^{2+} ions is reflected.

The magnetic properties of a large number of transition-metal complexes, organic radicals and metal-organic radical complexes have been studied so far, and the search for molecule-based magnetic materials has intensified in recent years.[1] In this field, a stable organic radical family, nitronyl nitroxide, is attracting much interest, because of potential ferromagnetic properties. Various nitronyl nitroxide derivatives have been found to exhibit ferromagnetic intermolecular interactions in their bulk crystals[2—14] since the discovery of the first pure organic ferromagnet, *p*-nitrophenyl nitronyl nitroxide.[15] Further, the nitronyl nitroxide has also been known to be a bidentate ligand for various transition and rare-earth metal ions. Ferromagnetic ground states have been observed in these complexes.[16—19]

Recently, we have embarked upon a study of *m*- and *p*-*N*-alkylpyridinium nitronyl nitroxide (4,4,5,5-tetramethyl-2-(1-methyl-3 or 4-pyridinio)-3-oxide-4,5-dihydro-1*H*-1-imidazolyloxyl) radical cations. We have already reported magneto-structural correlations in the I^- and ClO_4^- salts of *m*- and *p*-*N*-methylpyridinium nitronyl nitroxide (abbreviated as *m*- and *p*-MPYNN$^+$, respectively) (Scheme 1).[10,20,21] *m*-MPYNN$^+$$I^-$ and *m*-MPYNN$^+$$ClO_4^-$ are isostructural, in which *m*-MPYNN$^+$ forms a bond-alternated hexagonal lattice involving both ferromagnetic and antiferromagnetic interactions.[10] The I^- and ClO_4^- salts of *p*-MPYNN$^+$ exhibit quite different crystal structures: The crystal of *p*-MPYNN$^+$$I^-$ consists of a radical dimer with an antiferromagnetic interaction, while, in the crystal of *p*-MPYNN$^+$$ClO_4^-$, the *p*-MPYNN$^+$ cation is isolated by the ClO_4^- anion and

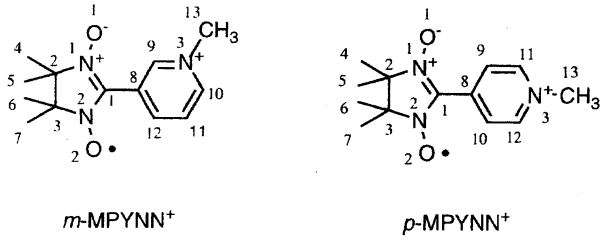

m-MPYNN$^+$ *p*-MPYNN$^+$

Scheme 1.

shows Curie paramagnetism.[20] The crystal structures and magnetic properties of *m*- and *p*-MPYNN$^+$ are expected to strongly depend on the counter anion. In this work we adopted the magnetic MCl_4^{2-} (M = Mn^{2+} ($S=5/2$) and Co^{2+} ($S=3/2$)) anions as the counter of *m*- and *p*-MPYNN$^+$ (Scheme 2). It is interesting to see the crystal structure caused by the insertion of MCl_4^{2-}, the d–π magnetic interaction, and how the difference in the metal ion of MCl_4^{2-} affects the bulk magnetism. We describe the structural and magnetic properties of the four salts: (*m*-MPYNN$^+$)$_2$$MnCl_4^{2-}$, (*m*-MPYNN$^+$)$_2$$CoCl_4^{2}$, (*p*-MPYNN$^+$)$_2$$MnCl_4^{2-}$, and (*p*-MPYNN$^+$)$_2$$CoCl_4^{2-}$.

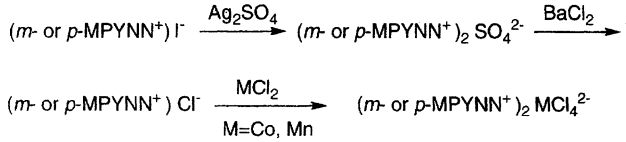

Scheme 2.

Experimental

Materials. The iodide salts of *m*-MPYNN$^+$ and *p*-MPYNN$^+$ were prepared by a reported method.[5,22] The iodide ion was replaced by chloride in the following procedure. To an aqueous solution of *p*- or *m*-MPYNN$^+$I$^-$ (1 g, 2.7 mmol) was added an excess amount of powdered silver sulfate. During stirring of 1 h the precipitation of silver iodide took place and the iodide ion was completely removed from the solution. To the filtrate, including *p*- or *m*-MPYNN$^+$ and SO_4^{2-}, was added a solution of barium chloride. After 1 h, precipitated barium sulfate was filtered off and the chloride salt was obtained by removing the solvent. A dry ethanol solution of *m*- or *p*- MPYNN$^+$Cl$^-$ (500 mg, 1.8 mmol) was added to a solution of $MnCl_2 \cdot 6H_2O$ (356 mg, 0.9 mmol) or $CoCl_2 \cdot 4H_2O$ (209 mg, 0.9 mmol), resulting in the immediate precipitation of a solid. The mixture was heated and a portion of hot ethanol was added until the precipitation dissolved. Slow evaporation of the solvent under a nitrogen atmosphere at room temperature led to crystallization of the MCl_4^{2-} salt. Elemental analyses gave, Found: C, 44.96; H, 5.67; N, 12.35; Cl, 20.72% for (*m*-MPYNN$^+$)$_2$MnCl$_4^{2-}$. Calcd: C, 44.91; H, 5.51; N, 12.09; Cl, 20.40%. Found: C, 42.14; H, 5.37; N, 11.69; Cl, 20.48% for (*m*-MPYNN$^+$)$_2$CoCl$_4^{2-}$. Calcd: C, 44.65; H, 5.48; N, 12.02; Cl, 20.28%. Found: C, 44.20; H, 5.68; N, 11.82; Cl, 19.93% for (*p*-MPYNN$^+$)$_2$MnCl$_4^{2-}$. Calcd: C, 44.91; H, 5.51; N, 12.09; Cl, 20.40%. and Found: C, 44.42; H, 5.56; N, 11.87; Cl, 19.43% for (*p*-MPYNN$^+$)$_2$CoCl$_4^{2-}$. Calcd: C, 44.65; H, 5.48; N, 12.02; Cl, 20.28%. The $MnCl_4^{2-}$ salts were rather air-sensitive in contrast to the stable $CoCl_4^{2-}$ salts.

Magnetic Measurements. Magnetic-susceptibility measurements were performed in the temperature range 3—280 K under a magnetic field of 0.5 T, using a Faraday balance.[23] Diamagnetic corrections were carried out, compensating for the diamagnetic susceptibilities which were estimated by assuming that the paramagnetic component follows the Curie law at high temperatures.

X-Ray Structure Determination. X-Ray diffraction data were collected on a Rigaku AFC-5 automatic four-circle diffractometer with graphite monochromatized Mo $K\alpha$ radiation at room temperature. The unit-cell parameters were derived by least-squares refinements of the setting angles of 25 representative reflections in the $20 < 2\theta < 25°$ range. The results for the *m*- and *p*-MPYNN$^+$ salts are shown in Tables 1 and 2, respectively. We carried out full data collection and analyses only on the stable $CoCl_4^{2-}$ salts of *m*- and *p*-MPYNN$^+$, because the $MnCl_4^{2-}$ salts were unstable and were indicated to be isostructural to the corresponding $CoCl_4^{2-}$ salts, respectively, as explained latter. During the collection, the intensities of three reflections were monitored as a check on the crystal stability. No loss of intensity was found for (*p*-MPYNN$^+$)$_2$CoCl$_4^{2-}$, although the intensity of (*m*-MPYNN$^+$)$_2$CoCl$_4^{2-}$ gradually decreased down to 90% of the original value at the end of the collection. This would be because of sample damage, presumably by air oxidation. The data of (*m*-MPYNN$^+$)$_2$CoCl$_4^{2-}$ were corrected according to the intensity decrease of the monitored reflections. Lorentz, polarization and absorption effects were also corrected for the two crystals. The structures were solved by a direct method with MULTAN and by subsequent difference Fourier syntheses. The non-hydrogen atoms were refined with anisotropic thermal parameters by the block-diagonal least-squares technique using UNICS III,[24] while those of the hydrogen atoms were not refined in order to avoid excessive parametrization. The experimental details are given in Tables 1 and 2. The final atomic parameters and equivalent isotropic thermal parameters for (*m*-MPYNN$^+$)$_2$CoCl$_4^{2-}$ and (*p*- MPYNN$^+$)$_2$CoCl$_4^{2-}$ are listed in Tables 3 and 4, respectively. The complete $F_o - F_c$ data are deposited as Document No. 69013 at the Office of the Editor of Bull. Chem. Soc. Jpn.

Results and Discussion

Crystal Structures. The unit-cell parameters of (*m*-MPYNN$^+$)$_2$CoCl$_4^{2-}$ and (*m*-MPYNN$^+$)$_2$MnCl$_4^{2-}$ are compared in Table 1, where the ratios between the corresponding cell parameters are also listed. The two salts crystallize into a *monoclinic* system with similar parameters. The cell volume of the $MnCl_4^{2-}$ salt is slightly larger than that of the $CoCl_4^{2-}$ salt, reflecting a larger ion radius of Mn^{2+} than that of Co^{2+}. Although we have not carried out an X-ray full structural analysis on the $MnCl_4^{2-}$ salt, it is considered to be isostructural to the $CoCl_4^{2-}$ salt on which the structural refinement was done, because the X-ray diffractions of the

Table 1. Crystal Data and Experimental Conditions for (*m*-MPYNN$^+$)$_2$CoCl$_4^{2-}$ and (*m*-MPYNN$^+$)$_2$MnCl$_4^{2-}$

	(*m*-MPYNN$^+$)$_2$CoCl$_4^{2-}$	(*m*-MPYNN$^+$)$_2$MnCl$_4^{2-}$	Ratio
Crystal system	*Monoclinic*		
a/Å	16.607(3)	16.741(3)	1.008
b/Å	13.501(2)	13.538(3)	1.003
c/Å	14.370(2)	14.398(2)	1.002
β/deg	90.43(2)	90.52(2)	1.001
V/Å^3	3221.8(9)	3262.9(9)	1.013
D(calcd)/g cm^{-3}	1.442	1.416	
Space group	$P2_1/c$		
Z	4		
μ/cm^{-1}	9.25		
Radiation	Mo $K\alpha$ (λ = 0.71073 Å) graphite monochromator		
2θ range/deg	4.0—50.0		
No. collected	5503		
No. obsd[a]	2244		
R	0.0906		
R_w	0.0907		

a) $|F_o| > 2.5\sigma(F_o)$.

Table 2. Crystal Data and Experimental Conditions for $(p\text{-MPYNN}^+)_2CoCl_4^{2-}$ and $(p\text{-MPYNN}^+)_2MnCl_4^{2-}$

	$(p\text{-MPYNN}^+)_2CoCl_4^{2-}$	$(p\text{-MPYNN}^+)_2MnCl_4^{2-}$	Ratio
	Triclinic		
a/Å	18.010(2)	18.112(4)	1.006
b/Å	20.040(2)	20.147(4)	1.005
c/Å	9.918(1)	9.969(2)	1.005
α/deg	93.22(2)	93.19(2)	0.9997
β/deg	99.17(1)	99.27(2)	1.001
γ/deg	109.89(1)	110.11(2)	1.002
V/Å^3	3299.4(8)	3347(1)	1.014
D(calcd)/g cm^{-3}	1.408	1.380	
Space group	$P\bar{1}$		
Z	4		
μ/cm^{-1}	9.04		
Radiation	Mo $K\alpha$ (λ = 0.71073 Å) graphite monochromator		
2θ range/deg	4.0—55.0		
No. collected	11154		
No. obsd[a)]	9169		
R	0.0672		
R_w	0.0688		

a) $|F_o| > 3.0\sigma(F_o)$.

$MnCl_4^{2-}$ salt in the range of $20 < 2\theta < 25°$ follow the same extinction rule as do those of the $CoCl_4^{2-}$ salt. Table 2 shows the crystal data of the two *p*-MPYNN$^+$ salts. They are also indicated to be isostructural, as the case of the *m*-MPYNN$^+$ salts. The crystal structures of the four salts depend little on MCl_4^{2-}.

Figure 1 shows a stereoview of the unit cell of $(m\text{-MPYNN}^+)_2CoCl_4^{2-}$, where one $CoCl_4^{2-}$ anion and two *m*-MPYNN$^+$ cations (molecules **A** and **B**) are crystallographically independent. The bond lengths and angles are listed in Table 5. The coordination of the cobalt(II) ion is slightly-distorted tetrahedral, and the $CoCl_4^{2-}$ anion is surrounded by four *m*-MPYNN$^+$ cations, resulting in the isolation of $CoCl_4^{2-}$. Figure 2(a) shows a projection of $CoCl_4^{2-}$ (i) onto the plane of the molecule **A**(ii), one of the four neighbors [symmetry operations: (i) x, y, z; (ii) $-x+1$, $-y$, $-z$].

There are short intermolecular, interatomic distances be-

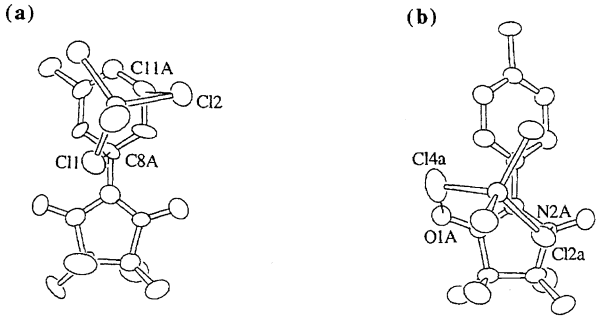

Fig. 2. Intermolecular arrangements between the organic radicals and $CoCl_4^{2-}$ in $(m\text{-MPYNN}^+)_2CoCl_4^{2-}$ (a) and $(p\text{-MPYNN}^+)_2CoCl_4^{2-}$ (b).

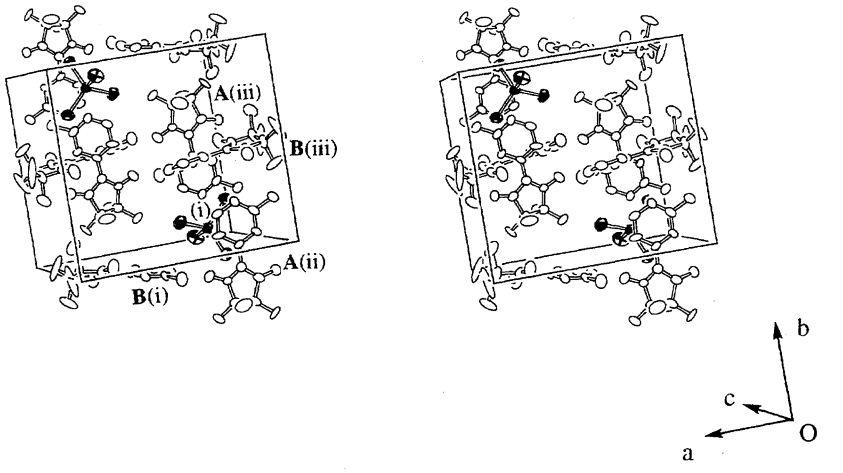

Fig. 1. Stereoview of the unit cell of $(m\text{-MPYNN}^+)_2CoCl_4^{2-}$. Symmetry operations: (i) x, y, z; (ii) $-x+1$, $-y$, $-z$; (iii) $-x+1$, $y+1/2$, $-z+1/2$.

Table 3. Atomic Coordinates ($\times 10^4$) and Equivalent Isotropic Thermal Parameters (Å$\times 10^2$) for (*m*-MPYNN$^+$)$_2$CoCl$_4^{2-}$

Atom	*x*	*y*	*z*	*B*(eq)
Co	3190(2)	1131(2)	2971(1)	3.8(.1)
Cl1	2706(3)	−257(4)	2307(3)	5.4(.1)
Cl2	4550(3)	1671(4)	2435(3)	5.9(.2)
Cl3	3448(4)	635(4)	4264(3)	6.5(.2)
Cl4	2114(4)	2367(4)	2921(4)	8.1(.2)
N1A	7980(9)	1365(9)	−133(8)	4.1(.4)
N2A	6474(8)	1222(8)	75(8)	3.6(.4)
N3A	8221(8)	−1824(9)	−122(7)	3.7(.4)
O1A	8831(7)	1175(8)	−241(7)	5.3(.4)
O1A	5670(7)	836(8)	181(8)	5.6(.4)
C1A	7250(10)	707(10)	−89(8)	3.2(.4)
C2A	7620(11)	2445(12)	−172(11)	4.9(.5)
C3A	6637(11)	2293(12)	242(11)	4.6(.5)
C4A	8313(12)	3111(14)	269(14)	6.7(.7)
C5A	7534(16)	2643(13)	−1087(11)	6.7(.7)
C6A	6706(15)	2351(15)	1183(11)	6.8(.7)
C7A	5857(12)	2938(13)	−96(14)	6.8(.7)
C8A	7350(10)	−360(9)	−194(8)	2.7(.4)
C9A	8166(9)	−820(10)	−33(9)	3.1(.4)
C10A	7519(11)	−2378(12)	−387(12)	5.4(.6)
C11A	6692(12)	−1928(11)	−551(12)	5.4(.6)
C12A	6572(12)	−905(12)	−456(10)	4.7(.5)
C13A	9119(12)	−2325(13)	139(12)	5.7(.6)
N1B	8548(8)	67(9)	2179(7)	3.4(.3)
N2B	8762(8)	−268(8)	3435(6)	2.9(.3)
N3B	5662(7)	−729(8)	2333(7)	3.1(.3)
O1B	8146(8)	218(10)	1503(7)	6.1(.4)
O2B	8591(8)	−518(9)	4155(6)	5.1(.4)
C1B	8099(10)	−209(10)	2855(8)	2.6(.4)
C2B	9557(10)	234(13)	2276(9)	4.5(.5)
C3B	9731(10)	−122(13)	3131(9)	4.1(.5)
C4B	9640(18)	1433(18)	2295(22)	13.0(1.3)
C5B	10100(13)	−87(31)	1628(11)	14.5(1.5)
C6B	10112(16)	−1242(16)	3050(18)	10.8(1.0)
C7B	10280(15)	452(23)	3716(11)	10.9(1.1)
C8B	7100(9)	−372(10)	2930(8)	2.7(.4)
C9B	6583(10)	−585(11)	2254(9)	3.3(.4)
C10B	5223(11)	−673(12)	3052(9)	3.9(.4)
C11B	5710(11)	−465(11)	3739(9)	3.8(.4)
C12B	6678(10)	−316(11)	3704(9)	3.7(.4)
C13B	5114(12)	−952(14)	1565(9)	5.3(.6)

tween the chlorine atoms and the pyridinium rings: 3.61(2) Å for Cl1(i)···C8A(ii) and 3.61(2) Å for Cl2(i)···Cl1A(ii). They could be caused by Coulombic attraction forces. The arrangement between the $CoCl_4^{2-}$ anion and the other three *m*-MPYNN$^+$ cations are similar to that in Fig. 2(a): the $CoCl_4^{2-}$ anion is located just on their pyridinium rings (not shown).

Furthermore, the crystal involves a short distance between **A** and **B** of *m*-MPYNN$^+$, whose arrangement is shown in Fig. 3. The two molecular planes are oriented nearly perpendicular to each other. The shortest intermolecular, interatomic distance is 3.01(2) Å for C1A(i)···O1B(i). The magnetic interaction derived from this contact is discussed later.

Table 4. Atomic Coordinates ($\times 10^4$) and Equivalent Isotropic Thermal Parameters (Å$\times 10^2$) for (*p*-MPYNN$^+$)$_2$CoCl$_4^{2-}$

Atom	*x*	*y*	*z*	*B*(eq)
Coa	2687(1)	5700(0)	3676(1)	3.3(.0)
Cl1a	4036(1)	5976(1)	3941(2)	4.9(.1)
Cl2a	2511(1)	6518(1)	5178(2)	5.2(.1)
Cl3a	2079(1)	4613(1)	4350(2)	5.0(.1)
Cl4a	2181(1)	5751(1)	1449(2)	6.0(.1)
Cob	2526(1)	836(0)	3861(1)	3.4(.0)
Cl1b	2235(1)	1567(1)	5365(2)	5.9(.1)
Cl2b	2119(1)	1047(1)	1682(2)	5.3(.1)
Cl3b	3843(1)	1000(1)	4168(2)	6.2(.1)
Cl4b	1761(1)	−266(1)	4297(2)	6.1(.1)
N1A	768(3)	6818(2)	2265(5)	2.9(.1)
N2A	598(3)	6805(3)	4405(5)	3.3(.2)
N3A	−963(3)	4232(2)	2216(5)	3.1(.1)
O1A	709(3)	6618(2)	1000(5)	4.1(.2)
O2A	415(3)	6577(3)	5519(5)	4.8(.2)
C1A	475(3)	6402(3)	3210(6)	2.9(.2)
C2A	1193(4)	7592(3)	2847(6)	3.3(.2)
C3A	904(4)	7591(3)	4252(7)	3.7(.2)
C4A	2106(4)	7745(4)	2963(8)	4.8(.2)
C5A	920(5)	8051(3)	1828(7)	4.3(.2)
C6A	161(5)	7826(4)	4192(9)	5.5(.3)
C7A	1571(5)	7982(4)	5516(8)	5.3(.3)
C8A	11(3)	5635(3)	2927(6)	2.8(.2)
C9A	181(4)	5215(3)	1946(7)	3.5(.2)
C10A	−631(4)	5336(3)	3598(7)	3.6(.2)
C11A	−328(4)	4502(3)	1592(7)	3.5(.2)
C12A	−1111(4)	4624(3)	3216(7)	3.5(.2)
C13A	−1516(4)	3470(3)	1763(7)	4.0(.2)
N1B	5469(3)	4374(3)	1841(5)	3.3(.2)
N2B	5150(3)	3214(3)	1542(6)	3.9(.2)
N3B	3589(3)	3555(3)	5261(5)	3.6(.2)
O1B	5524(3)	5003(2)	2284(5)	4.4(.2)
O2B	4884(4)	2552(3)	1702(6)	6.3(.2)
C1B	5028(4)	3752(3)	2243(7)	3.2(.2)
C2B	6014(4)	4266(3)	903(7)	3.5(.2)
C3B	5577(4)	3460(4)	371(7)	4.2(.2)
C4B	6849(4)	4440(4)	1836(8)	4.9(.3)
C5B	6058(5)	4772(4)	−209(8)	5.0(.3)
C6B	4893(6)	3320(5)	−915(8)	6.6(.3)
C7B	6144(6)	3040(4)	223(10)	6.1(.3)
C8B	4518(3)	3680(3)	3270(6)	3.1(.2)
C9B	4323(4)	4266(3)	3741(6)	3.3(.2)
C10B	4215(4)	3027(3)	3804(7)	3.8(.2)
C11B	3852(4)	4186(3)	4734(7)	3.5(.2)
C12B	3762(4)	2980(4)	4817(7)	4.1(.2)
C13B	3085(5)	3485(4)	6363(8)	4.8(.2)
N1C	690(3)	2034(3)	10824(5)	3.5(.2)
N2C	1586(4)	2522(3)	9575(6)	4.3(.2)
N3C	283(3)	−27(3)	7165(5)	3.4(.2)
O1C	108(3)	1587(3)	11242(5)	5.6(.2)
O2C	1991(5)	2621(3)	8629(8)	9.4(.3)
C1C	1004(4)	1917(3)	9740(6)	3.0(.2)
C2C	1133(4)	2772(3)	11607(7)	3.7(.2)
C3C	1688(4)	3145(3)	10606(7)	3.9(.2)
C4C	489(5)	3102(4)	11845(8)	5.0(.3)
C5C	1576(5)	2658(4)	12996(7)	4.9(.3)
C6C	2589(5)	3482(6)	11279(10)	7.2(.3)
C7C	1402(6)	3675(4)	9773(10)	6.4(.4)

Table 4. (Continued)

Atom	x	y	z	B(eq)
C8C	750(4)	1240(3)	8859(6)	3.0(.2)
C9C	23(4)	691(3)	8886(7)	3.5(.2)
C10C	1238(4)	1137(3)	7952(6)	3.4(.2)
C11C	−198(4)	61(3)	8022(7)	3.7(.2)
C12C	989(4)	494(3)	7111(7)	3.7(.2)
C13C	27(5)	−713(4)	6227(8)	5.1(.3)
N1D	4005(3)	98(3)	8171(6)	4.1(.2)
N2D	3181(3)	−928(3)	8601(6)	4.2(.2)
N3D	4247(3)	−1689(3)	4550(6)	3.8(.2)
O1D	4574(3)	537(3)	7714(6)	5.8(.2)
O2D	2808(4)	−1599(3)	8561(6)	6.7(.2)
C1D	3706(4)	−618(3)	7813(7)	3.6(.2)
C2D	3636(4)	335(4)	9282(7)	4.1(.2)
C3D	3008(5)	−393(4)	9522(8)	4.7(.2)
C4D	4327(6)	678(6)	10528(10)	8.7(.4)
C5D	3259(8)	859(7)	8672(15)	10.3(.6)
C6D	2126(5)	−475(6)	8950(15)	9.6(.5)
C7D	3143(9)	−583(6)	10991(10)	10.6(.6)
C8D	3916(4)	−983(3)	6695(7)	3.4(.2)
C9D	4060(4)	−654(4)	5502(7)	3.7(.2)
C10D	3950(4)	−1669(4)	6794(7)	4.2(.2)
C11D	4230(4)	−1020(4)	4441(7)	4.0(.2)
C12D	4124(4)	−2008(4)	5697(8)	4.3(.2)
C13D	4432(5)	−2072(4)	3378(9)	5.8(.3)

Table 5. Selected Bond Lengths (Å) and Angles (deg) for $(m\text{-MPYNN}^+)_2CoCl_4^{2-}$

$(m\text{-MPYNN}^+)_2CoCl_4^{2-}$			
Bond lengths			
Co–Cl1	2.282(5)	N2A–O2A	1.280(18)
Co–Cl2	2.273(6)	N2A–C1A	1.344(19)
Co–Cl3	2.277(6)	N1B–O1B	1.276(18)
Co–Cl4	2.277(8)	N1B–C1B	1.351(18)
N1A-O1A	1.263(18)	N2B–O2B	1.267(17)
N1A-C1A	1.377(20)	N2B–C1B	1.353(18)
Bond angles			
Cl1–Co–Cl2	109.5(2)	Cl3–Co–Cl4	110.9(2)
Cl1–Co–Cl3	105.3(2)	O1A–N1A–C1A	127.9(13)
Cl1–Co–Cl4	112.3(2)	O2A–N2A–C1A	124.6(13)
Cl2–Co–Cl3	109.2(2)	O1B–N1B–C1B	124.1(13)
Cl2–Co–Cl4	109.6(2)	O2B–N2B–C1B	123.3(12)

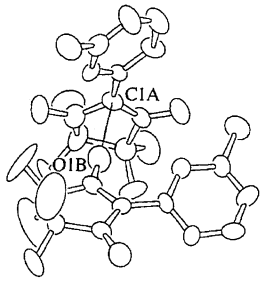

Fig. 3. Intermolecular arrangement of the *m*-MPYNN$^+$ dimer in $(m\text{-MPYNN}^+)_2CoCl_4^{2-}$.

Figure 4 shows a stereoview of the unit cell of $(p\text{-MPYNN}^+)_2CoCl_4^{2-}$, where two $CoCl_4^{2-}$ anions (molecules **a** and **b**) and four *p*-MPYNN$^+$ cations (molecules **A**—**D**) are crystallographically independent. The bond lengths and angles are listed in Table 6. The $CoCl_4^{2-}$ anions show slightly-distorted tetrahedral structures. Each $CoCl_4^{2-}$ is sandwiched by the two molecular planes of *p*-MPYNN$^+$. Figure 2(b) shows a projection of **a**(i) onto the molecular plane of **A**(i) [symmetry operation: (i) x, y, z]. The $CoCl_4^{2-}$ anion makes contact with the NO groups, with shorter intermolecular, interatomic distances of 3.653(7) Å for Cl 2a(i)···N2A(i) and 3.617(6) Å for Cl 4a(i)···O1A(i). The molecule **B**(ii) is located at the other side of **A**(i) with respect to **a**(i), where there is also a distance between **B**(ii) and the NO group of **a**(i) [symmetry operation: (ii) $-x+1, -y+1, -z+1$]. Further, **b**(i) of $CoCl_4^{2-}$ is sandwiched by the molecular planes of **C**(iii) and **D**(i) of *p*-MPYNN$^+$, having short distances to their NO groups [symmetry operation: (iii) $x, y, z-1$].

Magnetic Properties. The temperature dependence of the molar paramagnetic susceptibilities χ_p of $(m\text{-MPYNN}^+)_2MnCl_4^{2-}$ and $(m\text{-MPYNN}^+)_2CoCl_4^{2-}$ are

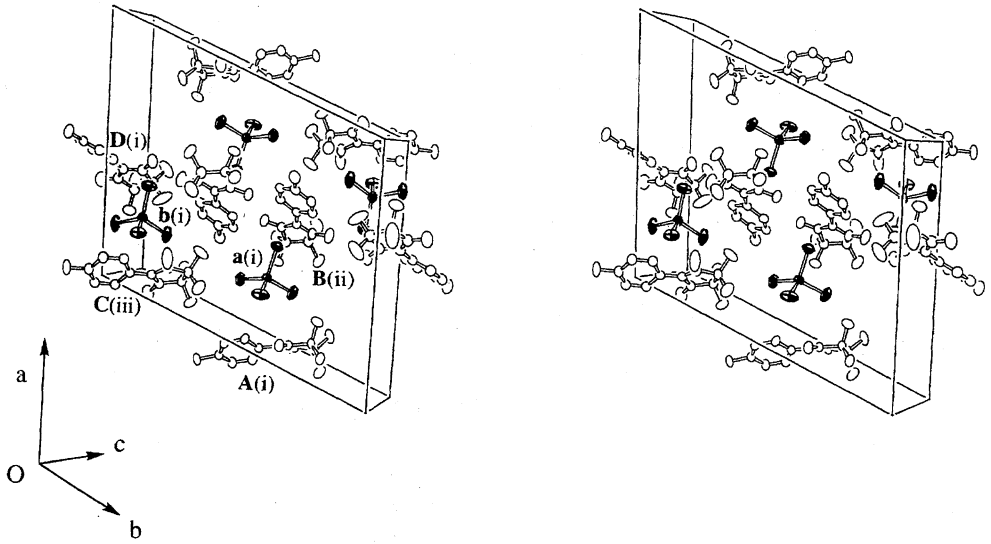

Fig. 4. Stereoview of the unit cell of $(p\text{-MPYNN}^+)_2CoCl_4^{2-}$. Symmetry operations: (i) x, y, z; (ii) $-x+1, -y+1, -z+1$; (iii) $x, y, z-1$.

Table 6. Selected Bond Lengths (Å) and Angles (deg) for (p-MPYNN$^+$)$_2$CoCl$_4^{2-}$

(p-MPYNN$^+$)$_2$CoCl$_4^{2-}$			
Bond lengths			
Coa–Cl1a	2.267(2)	N1B–O1B	1.277(8)
Coa–Cl2a	2.289(3)	N1B–C1B	1.351(8)
Coa–Cl3a	2.272(2)	N2B–O2B	1.277(9)
Coa–Cl4a	2.273(3)	N2B–C1B	1.348(9)
Cob–Cl1b	2.274(3)	N1C–O1C	1.270(8)
Cob–Cl2b	2.279(3)	N1C–C1C	1.336(8)
Cob–Cl3b	2.248(3)	N2C–O2C	1.262(11)
Cob–Cl4b	2.279(3)	N2C–C1C	1.345(9)
N1A–O1A	1.272(7)	N1D–O1D	1.269(9)
N1A–C1A	1.341(8)	N1D–C1D	1.352(9)
N2A–O2A	1.268(8)	N2D–O2D	1.277(9)
N2A–C1A	1.340(8)	N2D–C1D	1.335(9)
Bond angles			
Cl1a–Coa–Cl2a	105.6(1)	Cl2b–Cob–Cl4b	111.6(1)
Cl1a–Coa–Cl3a	111.5(1)	Cl3b–Cob–Cl4b	112.9(1)
Cl1a–Coa–Cl4a	109.1(1)	O1A–N1A–C1A	126.4(5)
Cl2a–Coa–Cl3a	106.0(1)	O2A–N2A–C1A	125.8(6)
Cl2a–Coa–Cl4a	112.8(1)	O1B–N1B–C1B	127.1(6)
Cl3a–Coa–Cl4a	111.6(1)	O2B–N2B–C1B	127.1(6)
Cl1b–Cob–Cl2b	108.5(1)	O1C–N1C–C1C	126.3(6)
Cl1b–Cob–Cl3b	113.3(1)	O2C–N2C–C1C	127.3(7)
Cl1b–Cob–Cl4b	101.8(1)	O1D–N1D–C1D	125.4(6)
Cl2b–Cob–Cl3b	108.6(1)	O2D–N2D–C1D	126.0(6)

shown in Fig. 5(a), in the form of χ_pT vs. T. Each χ_pT value at room temperature is explained as that of the non-interacting magnetic moments on the organic and inorganic ions. In this figure, the χ_pT plots of the two salts appear to be parallel: χ_pT increases with decreasing temperature down to 10 K, indicating a ferromagnetic interaction, but decreases below it. The two salts are concluded to involve a similar magnetic interaction without depending on the metal ions. Figure 5(b) shows χ_pT of the two p-MPYNN$^+$ salts. They show an opposite temperature dependence: χ_pT of (p-MPYNN$^+$)$_2$MnCl$_4^{2-}$ decreases with decreasing temperature, indicating an antiferromagnetic interaction, while that of (p-MPYNN$^+$)$_2$CoCl$_4^{2-}$ shows a ferromagnetic interaction. The magnetic interaction in the p-MPYNN$^+$ salts is seriously affected by the metal ions, whereas the magnetic properties of the m-MPYNN$^+$ salts depend little on MCl_4^{2-}.

In the low-temperature region below 4 K, decreases of χ_pT are commonly observed in the three ferromagnetic salts. There are two possible reasons: One is the zero field splitting on the metal ions; the other is an antiferromagnetic coupling between the ferromagnetic units. At this stage, however, it is hard to identify the reason.

The structural difference between the corresponding $CoCl_4^{2-}$ and $MnCl_4^{2-}$ salts is thought to be so small that we discuss the magneto-structural correlations based on the refined structures of the $CoCl_4^{2-}$ salts. From a structural viewpoint, a crucial difference between the m- and p-MPYNN$^+$ salts is the position of the MCl_4^{2-} anion with respect to the molecular plane of the organic radicals. As shown in Fig. 2,

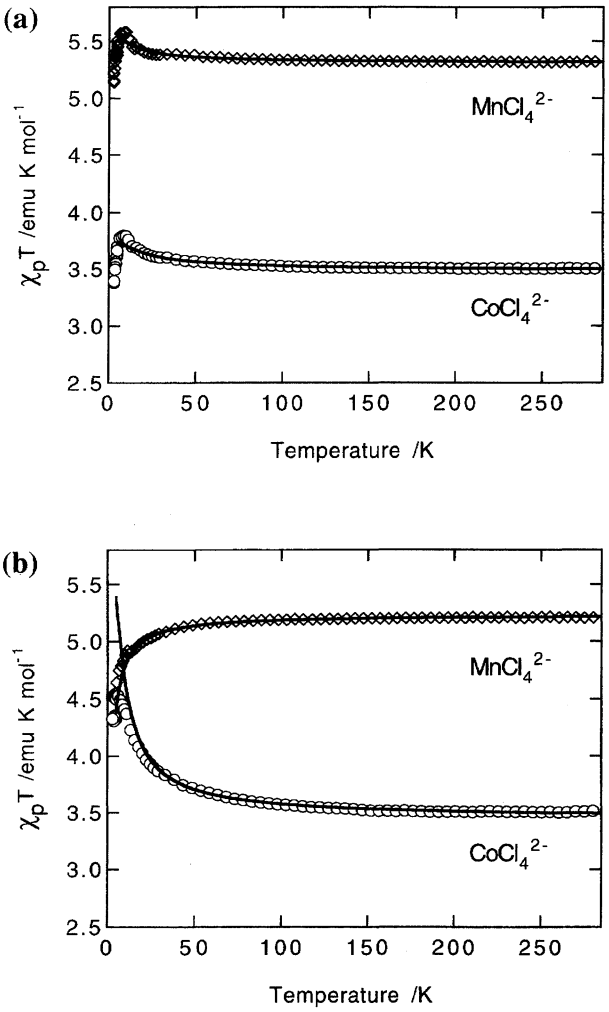

Fig. 5. Temperature dependence of the paramagnetic susceptibilities of (m-MPYNN$^+$)$_2$MCl$_4^{2-}$ (a) and (p-MPYNN$^+$)$_2$MCl$_4^{2-}$ (b). The solid curves are the theoretical ones. See the text.

in the crystal of (m-MPYNN$^+$)$_2$MCl$_4^{2-}$, the arrangement is formed by the distance between MCl_4^{2-} and the pyridinium ring; there is no short distance between MCl_4^{2-} and the NO groups, while the crystals of (p-MPYNN$^+$)$_2$MCl$_4^{2-}$ involve the latter contact. The SOMO of the nitronyl nitroxide is localized on the two NO groups, making a node on the α-carbon bridging the two NO groups, and has little population in the aromatic substituent, i.e. the pyridinium ring in this case.[25] The arrangement in the m-MPYNN$^+$ salts, therefore, means only a small overlap of the SOMO of m-MPYNN$^+$ with the magnetic d orbitals of MCl_4^{2-}, suggesting the absence of a magnetic interaction between them. For this reason, the observed ferromagnetic interactions in the m-MPYNN$^+$ salts are expected to operate not between m-MPYNN$^+$ and MCl_4^{2-}, but between the organic radicals shown in Fig. 3. This is consistent with the fact that the magnetic interaction in (m-MPYNN$^+$)$_2$MCl$_4^{2-}$ does not depend on MCl_4^{2-}. The intermolecular contact in the m-MPYNN$^+$ dimer is between the NO group and the α-carbon. This arrangement indicates a nearly orthogonal relation between

the two SOMOs in spite of the short distance between them, which satisfies the requirement for the ferromagnetic intermolecular interaction.[25] In fact, similar arrangements have been observed in the ferromagnetic crystals of pyrimidinyl nitronyl nitroxide[8] and the lithium salt of *p*-benzoic acid nitronyl nitroxide.[9]

The temperature dependence of χ_p can be well interpreted as the sum of the ferromagnetic contribution from the *m*-MPYNN$^+$ dimer and the Curie paramagnetic contribution from the MCl_4^{2-} anion, using

$$\chi_p = \frac{2N_A g_1^2 \mu_B^2}{k_B T\{3+\exp(-2J/k_B T)\}} + \frac{N_A g_2^2 \mu_B^2}{3k_B T} S(S+1), \quad (1)$$

where J is the coupling constant in the ferromagnetic dimer, g_1 and g_2 are the g factors for the radical and the metal ion, respectively, N_A is Avogadro's constant, μ_B is the Bohr magneton, k_B is the Boltzmann constant and S is the spin quantum number of the metal ion. Using data above 30 K, the theoretical best fits are obtained with $J/k_B=8.2$ K, $g_1=2.00$ (fixed), and $g_2=2.04$ for the $MnCl_4^{2-}$ salt, and $J/k_B=12.4$ K, $g_1=2.00$ (fixed), and $g_2=2.41$ for the $CoCl_4^{2-}$ salt. The solid curves in Fig. 5(a) are theoretical ones, and explain the observed behavior above 30 K.

In the crystals of (*p*-MPYNN$^+$)$_2MCl_4^{2-}$, on the other hand, there is a short distance between the MCl_4^{2-} anion and the NO group. This means an overlap between the magnetic d orbitals and the SOMO of the organic radical, which would be a dominant factor in realizing bulk magnetism. Namely, the magnetic interaction between *p*-MPYNN$^+$ and MCl_4^{2-} is considered to change from antiferromagnetic to ferromagnetic by switching the metal ion in MCl_4^{2-} from Mn^{2+} to Co^{2+}. Since there is little difference in the crystal structure between (*p*-MPYNN$^+$)$CoCl_4^{2-}$ and (*p*-MPYNN$^+$)$_2MnCl_4^{2-}$, the difference in the magnetic interaction would originate in the electronic structures of $MnCl_4^{2-}$ and $CoCl_4^{2-}$.

Figure 6 shows the electronic configurations of the divalent metal ions in a tetrahedral ligand field and the nitronyl nitroxide radical. The Mn^{2+} and Co^{2+} ions are in the $S=5/2$ and 3/2 ground states, respectively. We thus assume a charge-transfer (CT) interaction from one of the 3d orbitals of the metal ion to the SOMO of the organic radical. A magnetic interaction between the $S=5/2$ spin on Mn^{2+} and the $S=1/2$ spin on *p*-MPYNN$^+$ results in either an $S=3$ or 2 spin state. However, the former one is forbidden in the CT interaction, because every frontier orbital is singly occupied in the ground state, so that the CT inevitably decreases the spin multiplicity down to $S=2$, as shown in Fig. 6(a). The resonance with the $S=2$ CT excited state stabilizes an antiferromagnetic interaction. In the case of the $CoCl_4^{2-}$ salt, on the other hand, both ferromagnetic ($S=2$) and antiferromagnetic ($S=1$) excitations are possible (see Fig. 6(b)). It

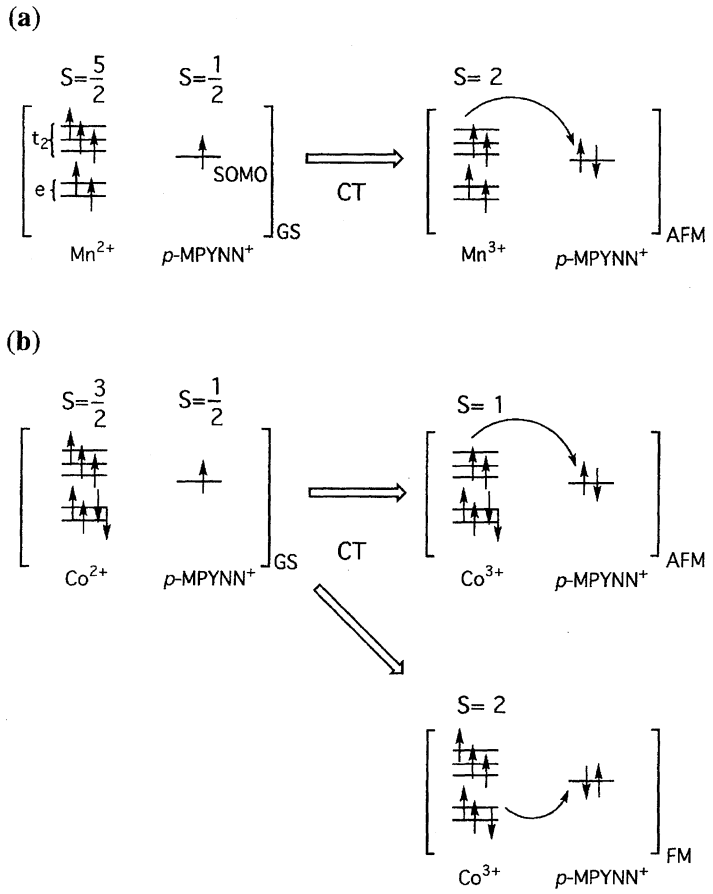

Fig. 6. Electronic structures of the MCl_4^{2-} anions and the nitronyl nitroxide radical.

is worth noting here that a metal ion in a tetrahedral ligand field always prefers a high spin ground state, because the electronic repulsion in the paired electrons is larger than the splitting energy of the tetrahedral ligand field. This means that a transfer which leaves a higher spin multiplicity in the Co^{3+} (namely $S=2$) is energetically advantageous. The admixture of the $S=2$ CT excited state results in a stabilization of the ferromagnetic interaction between the $S=3/2$ Co^{2+} ion and the $S=1/2$ organic radical. For these, the difference in the magnetic interaction between the $MnCl_4^{2-}$ and $CoCl_4^{2-}$ salts can be qualitatively understood based on the electronic structures of the metal ions.

Since MCl_4^{2-} is sandwiched by two *p*-MPYNN$^+$ cations in the crystals of (*p*-MPYNN$^+$)$_2MCl_4^{2-}$, we apply a three-spin mode, $H=-2J[\boldsymbol{S}_1\cdot\boldsymbol{S}_2+\boldsymbol{S}_2\cdot\boldsymbol{S}_3]$, to the magnetic systems in the *p*-MPYNN$^+$ salts, where $\boldsymbol{S}_1$ and $\boldsymbol{S}_3$ are spin operators for the two *p*-MPYNN$^+$ cations, $\boldsymbol{S}_2$ is that for the metal ion, and J is the coupling constant. For $S_1=S_3=1/2$, the expression for χ_p is[26]

$$\chi_p=\frac{N_A g^2\mu_B^2}{k_B T}\times\left\{\frac{a_1(S_2)\exp(-(2S_2+2)J/k_BT)}{(2S_2-1)\exp(-(2S_2+2)J/k_BT)}\right.$$
$$\left.\frac{+a_2(S_2)(\exp(-2J/k_BT)+1)+a_3(S_2)\exp(2S_2J/k_BT)}{+(2S_2+1)(\exp(-2J/k_BT)+1)+(2S_2+3)\exp(2S_2J/k_BT)}\right\}, \quad (2)$$

where g is the average g factor over the three spins, $S_2=3/2$, $a_1=1/2$, $a_2=5$, $a_3=35/2$ for (*p*-MPYNN$^+$)$_2CoCl_4^{2-}$, and $S_2=5/2$, $a_1=5$, $a_2=35/2$, $a_3=42$ for (*p*-MPYNN$^+$)$_2MnCl_4^{2-}$. Using data above 30 K, the theoretical best fits are obtained with $J/k_B=-0.72$ K and $g=2.02$ for the $MnCl_4^{2-}$ salt, and $J/k_B=3.6$ K and $g=2.29$ for the $CoCl_4^{2-}$ salt. The theoretical curves in Fig. 5(b) quantitatively explain the magnetic behavior of the *p*-MPYNN$^+$ salts above 30 K.

Conclusions

We have studied the structural and magnetic properties of the four salts: (*m*-MPYNN$^+$)$_2MnCl_4^{2-}$, (*m*-MPYNN$^+$)$_2CoCl_4^{2-}$, (*p*-MPYNN$^+$)$_2MnCl_4^{2-}$, and (*p*-MPYNN$^+$)$_2CoCl_4^{2-}$. Their crystal structures are found to be governed by only the organic radical cations. A crucial difference in the mutual arrangement between the MCl_4^{2-} anion and the organic radical cation is that the MCl_4^{2-} is located just on the pyridinium ring of *m*-MPYNN$^+$ in the crystals of (*m*-MPYNN$^+$)$_2MCl_4^{2-}$, while MCl_4^{2-} makes contact with the NO groups of *p*-MPYNN$^+$ in (*p*-MPYNN$^+$)$_2MCl_4^{2-}$. The two *m*-MPYNN$^+$ salts exhibit ferromagnetic behavior which is attributable to the *m*-MPYNN$^+$ dimer formed by the intermolecular distance between the NO group and the α-carbon. On the other hand, the two *p*-MPYNN$^+$ salts exhibit an opposite magnetic behavior: (*p*-MPYNN$^+$)$_2CoCl_4^{2-}$ and (*p*-MPYNN$^+$)$_2MnCl_4^{2-}$ are ferro- and antiferromagnetic, respectively. The opposite magnetic interactions in the *p*-MPYNN$^+$ salts are well understood in terms of the CT interaction between MCl_4^{2-} and *p*-MPYNN$^+$, in which the electronic structures of the Co^{2+} and Mn^{2+} ions are reflected.

This work was supported by a Grant-in-aid for Scientific Research from the Ministry of Education, Science and Culture. Support from New Energy and Industrial Technology Development Organization (NEDO) is also acknowledged.

References

1) J. S. Miller and A. J. Epstein, *Angew. Chem., Int. Ed. Engl.*, **33**, 385 (1994).
2) H. Wang, D. Zhang, M. Wan, and D. Zhu, *Solid State Commun.*, **85**, 685 (1993).
3) P. Turek, K. Nozawa, D. Shiomi, K. Awaga, T. Inabe, Y. Maruyama, and M. Kinoshita, *Chem. Phys. Lett.*, **180**, 327 (1991).
4) T. Sugano, M. Tamura, M. Kinoshita, Y. Sakai, and Y. Ohashi, *Chem. Phys. Lett.*, **200**, 235 (1992).
5) K. Awaga, T. Inabe, Y. Maruyama, T. Nakamura, and M. Matsumoto, *Chem. Phys. Lett.*, **195**, 21 (1992).
6) E. Hernàndez, M. Mas, E. Molins, C. Rovira, and J. Veciana, *Angew. Chem., Int. Ed. Engl.*, **32**, 882 (1993).
7) M. Tamura, D. Shiomi, Y. Hosokoshi, N. Iwasawa, K. Nozawa, M. Kinoshita, H. Sawa, and R. Kato, *Mol. Cryst. Liq. Cryst.*, **232**, 45 (1993).
8) F. L. d. Panthou, D. Luneau, J. Laugier, and P. Rey, *J. Am. Chem. Soc.*, **115**, 9095 (1993).
9) K. Inoue and H. Iwamura, *Chem. Phys. Lett.*, **207**, 551 (1993).
10) K. Awaga, T. Okuno, A. Yamaguchi, M. Hasegawa, T. Inabe, Y. Maruyama, and N. Wada, *Phys. Rev. B*, **49**, 3975 (1994).
11) K. Awaga, A. Yamaguchi, T. Okuno, T. Inabe, T. Nakamura, M. Matsumoto, and Y. Maruyama, *J. Mater. Chem.*, **4**, 1377 (1994).
12) T. Sugawara, M. M. Matsushita, A. Izuoka, N. Wada, N. Takeda, and M. Ishikawa, *J. Chem. Soc., Chem. Commun.*, **1994**, 1723.
13) T. Akita, Y. Mazaki, K. Kobayashi, N. Koga, and H. Iwamura, *J. Org. Chem.*, **60**, 2092 (1995).
14) J. Cirujeda, L. E. Ochando, J. M. Amigó, C. Rovira, J. Rius, and J. Veciana, *Angew. Chem., Int. Ed. Engl.*, **34**, 55 (1995).
15) M. Kinoshita, P. Turek, M. Tamura, K. Nozawa, D. Shiomi, Y. Nakazawa, M. Ishikawa, M. Takahashi, K. Awaga, T. Inabe, and Y. Maruyama, *Chem. Lett.*, **1991**, 1225.
16) D. Gatteschi, J. Laugier, P. Rey, and C. Zanchini, *Inorg. Chem.*, **26**, 938 (1987).
17) A. Caneschi, D. Gatteschi, P. Rey, and R. Sessoli, *Inorg. Chem.*, **27**, 1756 (1988).
18) A. Caneschi, D. Gatteschi, J. P. Renard, P. Rey, and R. Sessoli, *Inorg. Chem.*, **28**, 2940 (1989).
19) C. Benelli, A. Caneschi, D. Gatteschi, and R. Sessoli, *Inorg. Chem.*, **32**, 4797 (1993), references are therein.
20) A. Yamaguchi, K. Awaga, T. Inabe, T. Nakamura, M. Matsumoto, and Y. Maruyama, *Chem. Lett.*, **1993**, 1443.
21) K. Awaga, T. Inabe, T. Nakamura, M. Matsumoto, and Y. Maruyama, *Mol. Cryst. Liq. Cryst.*, **232**, 69 (1993).
22) K. Awaga, T. Inabe, U. Nagashima, T. Nakamura, M. Matsumoto, Y. Kawabata, and Y. Maruyama, *Chem. Lett.*, **1991**, 1777.
23) K. Awaga and Y. Maruyama, *Chem. Mater.*, **2**, 535 (1990).
24) T. Sakurai and K. Kobayashi, *Rep. Inst. Phys. Chem. Res. (Jpn.)*, **55**, 69 (1979).
25) K. Awaga, T. Inabe, U. Nagashima, and Y. Maruyama, *J. Chem. Soc., Chem. Commun.*, **1989**, 1617.
26) D. Sekutowski, R. Jungst, and G. D. Stucky, *Inorg. Chem.*, **17**, 1848 (1978).